# Tracking high molecular weight polymer interdiffusion on a SERS-based platform

## Carla D. Mana and J. Pablo Tomba*

We describe the implementation of an experimental setup based on Surface Enhanced Raman Spectroscopy (SERS) to investigate polymer interdiffusion. Ultra-thin bilayer films of deuterated polystyrene (dPS) and polystyrene (PS) are placed in contact onto SERS-active gold substrates with inverted square-base pyramidal geometry and subsequently annealed. Initially, the Raman spectrum shows only spectral features of the polymer adjacent to the substrate. Upon annealing, Raman bands of the polymer located far from the substrate start to emerge, an indication of chain diffusion into the substrate hotspot and mixing between polymer layers. The kinetics of the process is consistent with transport of polymer chains in nanometer scale, with diffusion coefficients in the range $10^{-13} - 10^{-15}$ cm$^2$/s. The temperature response of the process is characterized by an activation energy of $48.93 \pm 1.5$ kcal/mol, in excellent agreement with earlier experiments. SERS experiments provide a powerful and reliable experimental platform to characterize polymer interdiffusion without the need of chemical labeling, with several prospective applications to the study of chain dynamics in advanced polymer-based nanocomposite materials. Copyright © 2016 John Wiley & Sons, Ltd.

Additional supporting information may be found in the online version of this article at the publisher's web site.

Keywords: polymer interdiffusion; ultrathin films; SERS; Klarite; plasmon

## Introduction

The study of chain diffusion has been a central topic in the agenda of polymer science for fundamental reasons[1,2] as well as for its prominent role in several technologies such as welding, adhesion, coating, blending or lithography. Chain dynamics controls the time required for interpenetration of polymer chains and their eventual entanglement, a fundamental mechanism responsible for the adhesive strength growth in welding between polymer slabs, the mechanical consolidation in polymer latex films or the time required for a block copolymer to achieve an ordered structure.

For high molecular weight polymers, characteristic diffusion distances that define the interfacial structure are in the range of tens to hundreds of nanometers. Several techniques which high-spatial resolution ($<100$ nm) have been employed to investigate the topic, such as Forward Recoil Spectrometry,[3] Nuclear Reaction Analysis[4] or Fluorescence Resonance Energy Transfer,[5] along with many others recently developed.[6,7] With these techniques, diffusion coefficients below $10^{-14}$ cm$^2$/s have been typically measured. The drawback of these techniques is that they typically require chemical labeling to improve contrast thus complicating sample preparation. Micro-spectroscopies can overcome this limitation but at the cost of sacrificing spatial resolution and consequently the accessible range of diffusion coefficients to be measured. For instance, confocal Raman microscopy is naturally sensitive to the structure of each polymer chain, but its moderate diffraction-limited spatial resolution on the order of laser wavelength (300–800 nm)[8] limits the range of diffusion coefficients to be measured to values above $10^{-11}$ cm$^2$/s.[9,10]

The effect of local amplification of Raman signal by rough metals is the base for some remarkable techniques such as tip enhanced or surface enhanced Raman spectroscopies (TERS, SERS). The possibility of probing a reduced sample volume is very promising for the application to studies of chain diffusion. Recent work has reported the application of TERS to the characterization of phase structure of a polymer blend,[11] with a lateral resolution down to 50 nm.[12] The disadvantage of TERS is that it requires somewhat complex instrumentation, typically, an atomic force microscope coupled to a Raman spectrometer, besides the fact that the probing mode of TERS (lateral) is not the most adequate to dynamically probe a very thin interface. On the other hand, SERS can be performed in conventional Raman microscopes, but the complexity arises in the choice of a proper substrate for the desired application. The potential of the technique was demonstrated years ago by Boerio, who reported measurements of surface enrichment in polymer blends using colloidal silver as active substrate.[13] The recent advances in production technologies of engineered SERS substrates, as shown by the several commercial products currently found in the market, have opened up opportunities to develop new applications for the technique.

We describe the application of a SERS-based configuration to track chain diffusion at a polymer–polymer interface. In this preliminary work, we study the deuterated polystyrene (dPS)/polystyrene (PS) polymer pair. Molecular weights employed are well above that required for entanglements, anticipating diffusion distances on the scale of tens of nanometers. SERS of bilayered dPS/PS films is

* Correspondence to: J. Pablo Tomba, Institute of Materials Science and Technology (INTEMA), National Research Council (CONICET), University of Mar del Plata, Juan B. Justo 4302, 7600 Mar del Plata, Argentina.
E-mail: jptomba@fi.mdp.edu.ar

Institute of Materials Science and Technology (INTEMA), National Research Council (CONICET), University of Mar del Plata, Juan B. Justo 4302, 7600 Mar del Plata, Argentina

measured on engineered substrates with a structure of inverted pyramids using a conventional Raman microscope. Polymer diffusion is promoted by annealing the system above the glass transition temperatures of the polymers. Changes in spectral features are correlated with diffusion rates with the aim of establishing a quantitative base for polymer diffusion characterization. The influence of sample geometry, annealing time and temperature on diffusion rates are analyzed. Overall, the results indicate that the experiment is able to provide values of diffusion coefficients without precedent for conventional Raman microscopy.

## Experimental

### Materials

The neat polymers used to prepare bilayer samples were deuterated polystyrene (dPS) and polystyrene (PS). Both samples dPS ($M_w = 236\,500$) and PS ($M_w = 228\,000$), nearly monodisperse ($M_w/M_n < 1.05$), were purchased from Polymer Source. Glass transition temperatures ($T_g$), as measured by Differential Scanning Calorimetry at 10 °C/min heating rates, were close to 100 °C for both polymers.

The bilayer system studied was supported onto commercial SERS substrates (Klarite 313, Renishaw Diagnostics). The substrate was designed to obtain optimum enhancing signal when irradiated at 633 and 785 nm.[14] It was provided as a rectangular chip of $6 \times 10\ mm^2$, composed by two parts: one is a flat layer of gold on flat silicon (inactive area) and the other is a nanostructured silicon surface coated with a 300-nm layer of gold (active area). The active area ($4 \times 4\ mm^2$) is a regular array of inverted pyramid depressions, as shown in Fig. 1(A).

### Specimen preparation for diffusion experiments

Thin polymer films were prepared by spin-coating from dilute solutions in toluene. Film thickness was controlled by adjusting the concentration of the solution used, the angular velocity and the time step setup, based on previous protocols developed in the group. The resulting films had a thickness of $80 \pm 5$ nm, as measured onto glass substrates with a KLA Tencor 100 profilometer.

Polymer bilayers were prepared as follows. First, a thin film of one of the polymers was deposited onto the active SERS substrate by spin coating. Separately, a thin film of the other polymer was deposited by the same technique but onto a water-soluble potassium bromide (KBr) substrate. KBr was then removed with water to obtain a free standing film, which was subsequently deposited onto the first one. Bilayer films onto SERS substrate were left under vacuum at 40 °C for 1 day to remove solvent traces.

Diffusion between PS and dPS was promoted by thermal treatment under nitrogen atmosphere at several temperatures above their glass transition, using a Linkam THMS 600 hot stage.

### Raman measurements

Raman spectra were taken *in situ* with a Renishaw inVia Reflex Raman microscope equipped with a charge-coupled device (CCD) detector ($1040 \times 256$ pixels) using a long-distance objective Leica 50× (NA: 0.55). A diode laser of 785 nm was used in combination with a grating of 1200 slits/mm. An instrumental filter was used to reduce the incident power to 10%; actual laser powers measured onto the sample were below 7.5 mW. Confocality was achieved by tuning the pixel binning of the spatial dimension of the CCD and the aperture of the spectrograph entrance slit; values of 6 pixels
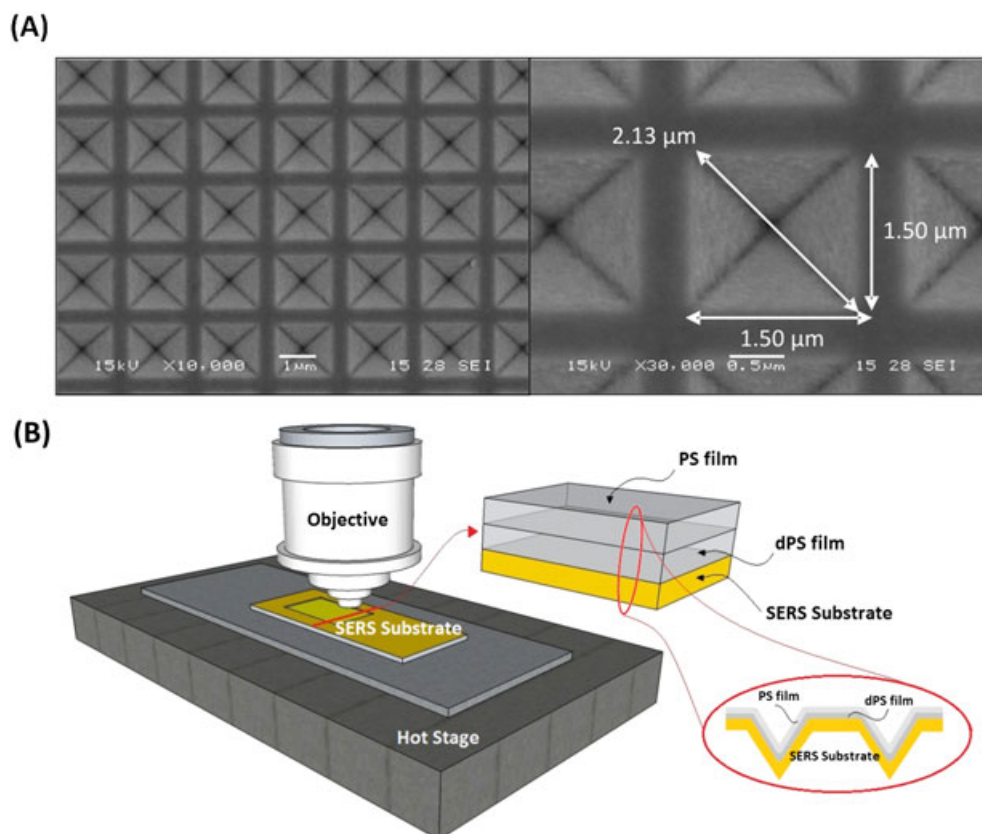


**Figure 1.** (A) SEM image of the active area of the Klarite substrate. (B) Sketch of the experimental setup.

and 65-μm slit opening were used. The lateral resolution under these instrumental conditions was measured by lateral scanning of the edge of a polished silicon wafer and by recording the intensity of the 520 cm$^{-1}$ silicon band; a value of 15 μm was obtained from the width of the bell-shaped curve at its half maximum. The acquisition time for each spectrum was 2 s with five accumulations. Spectra were taken at six different spots in steps of 2 μm on the sample and the results averaged.

A calibration curve was built to obtain polymer weight fractions from the Raman spectra. Homogeneous polymer blends containing different proportions of PS and dPS were prepared from dissolution in a common solvent (benzene) followed by freeze drying. Raman spectra for pure components and their blends of known composition were measured at room temperature. To obtain polymer compositions, the linear decomposition method was applied. The method computes individual PS and dPS contributions to the global blend spectrum and calculates the blend composition from the relative contributions and the calibration curve.[15]

A sketch of the experimental design is shown in Fig. 1(B). Diffusion specimens were mounted on the hot stage, subsequently attached to the stage of the Raman microscope. The specimen is annealed at a pre-established temperature while Raman spectra are periodically acquired, always keeping the focus on the surface of the active area of the SERS substrate. Figure 1(A) shows a SEM image of the SERS substrate. The manufacturer reports that the lateral dimension of the squared-based pyramidal pits is 1.5 μm, which agrees with that of the image, and that the pyramid height is about 1 μm.

## Results and discussion

Figure 2 shows conventional Raman spectra of the neat polymers, dPS and PS, and that of a solution of them with a composition of 70 wt% PS. The most noticeable bands at 960 cm$^{-1}$ and 1000 cm$^{-1}$ have been ascribed to aromatic in plane C–H (C–D in the case of dPS) deformation vibrations.[16] This difference in the spectral profiles generates the contrast between components necessary to follow the transport of polymer chains by SERS. The
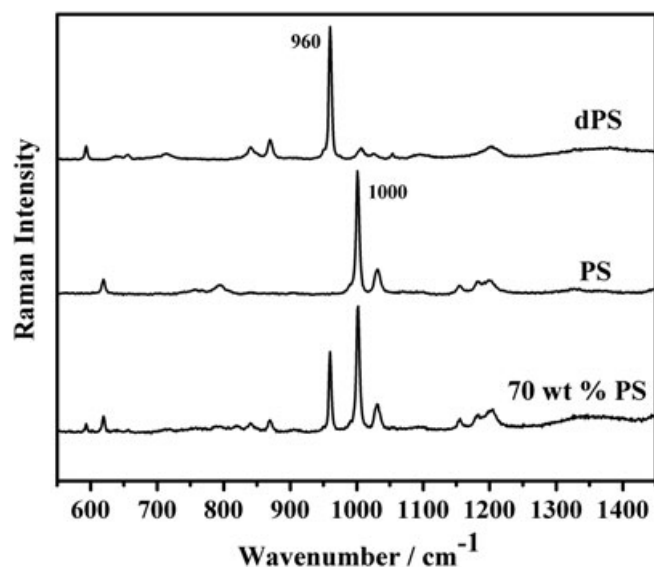
blend spectrum shows both 960 cm$^{-1}$ and 1000 cm$^{-1}$ Raman bands, with a predominance of the 1000 cm$^{-1}$ contribution giving the higher proportion of the PS component in the blend. This and others blends were used as with calibration purposes to translate the spectral information to weight composition. The analysis indicated that Raman cross sections of dPS and PS components were similar, which anticipates that a 50 wt% blend ought to show tracer peaks with similar intensity.

Figure 3 shows a series of Raman spectra of thin films. The spectrum at the top corresponds to that obtained from an 80-nm-thick dPS film deposited onto glass. The Raman spectrum of dPS was undetectable, and the broad band seen corresponds to the glass substrate. We conclude that an 80-nm-thick dPS film does not provide enough scattering to be detected by conventional Raman. The spectrum at the middle corresponds to a dPS film, 80 nm thick, but deposited onto the SERS substrate. In our acquisition conditions, the lateral dimensions of the laser spot is about 15 μm, much larger than those of a single pyramidal cavity, so data correspond to an average over about 56 pyramids. The clear spectral features of dPS observed corroborate the amplification of Raman signal produced by the substrate. Possible dewetting or poor contact between the hydrophobic polymer and the metallic substrate, effects that might be expected giving the nature of them, is not enough to prevent the acquisition of clear spectral data. The SERS spectrum was identical to that obtained from the thick films shown in Fig. 2, indicating that either there are not orientation effects of polymer chains relative to the gold substrate surface or the hotspot is large enough to include many unoriented chains from the film bulk that overwhelm those oriented. We conclude this by the lack of bands related to ring-mode contributions in Figs 2 and 3, which provide information about the orientation of polystyrene's ring relative to gold surface according to Anema et al.[17]

The spectrum at the bottom of Fig. 3 shows the Raman spectrum of a composite film, that is, the 80-nm-thick dPS film deposited onto Klarite, with a second 80-nm-thick PS film on top of it. To allow the PS film at the top to relax and to be in intimate contact with that of dPS on the bottom, a short thermal treatment (120 °C, 5 min) was applied. Remarkably, the SERS spectrum of the bilayer mostly shows spectral features of dPS, whereas those of PS are almost totally absent. This selective amplification indicates that the
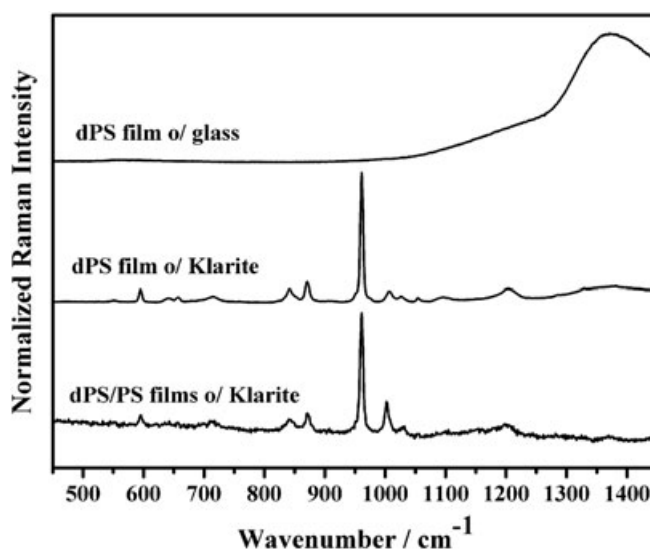


**Figure 2.** Conventional Raman spectra of pure dPS, PS and of a PS–dPS blend.



**Figure 3.** Raman spectra of thin films.

dimensions of the hotspot or detection zone of the substrate are actually below the nominal thickness of the dPS film, informed to be about 80 nm. This result is consistent with numerical simulations of hotspot localization carried out by other groups on this type of substrate geometry.[18,19] Vernon *et al.* simulated an infinitely long groove as a simplified 2D model of the inverted squared-based pyramid structure; these simulations showed that the maximum electric field reinforcement is given at the groove tip.[18] However, a more realistic 3D model of a single square-based pyramidal pit shows that the region of maximum field reinforcement is displaced from the tip and actually placed above it.[18,19] Also, Li *et al.* have shown that the field distribution in the pyramidal pit was not affected by the pits around it, but its intensity increased in the pit array by coupling effect between surface plasmons.[19] None of these simulations have considered the effect of the polymer layer on the laser–metal interaction, an issue that will be addressed in future simulations of the plasmonic effect of this specific system. We conclude that is in the cavities of the pyramid, more than at their tips, where the amplification of the electromagnetic field is more intense, between a few and 80 nm from the tip.

The reproducibility of Raman signal in SERS experiments was an issue also addressed. On one hand, we tracked intensity variations in thin films over different spots of the SERS substrate. With this aim, the intensity of peak at 1000 cm$^{-1}$ (PS) was measured over an area of about $100 \times 100$ μm$^2$ of Klarite. Overall, we found that collected intensities values were very homogeneous, with variations below 10%, see Fig. S1 (Supporting Information). Another experiment carried out consisted in tracking intensity variations with time at high temperature (185 °C), with the aim of looking for possible degradation of either the substrate or the polymer. Substrate degradation is particularly relevant to this experiment as it would possibly imply variations of the dimensions of the hotspot of the substrate. Figure S2 (Supporting Information) shows Raman spectra of PS and dPS films acquired at different annealing times at 185 °C. It is seen that overall spectral intensity does not change substantially, a good indication that substrate properties have remained essentially invariant. It is observed, however, broad bands at 1400 and 1600 cm$^{-1}$ that might indicate some polymer degradation.[14,20] However, that contribution is actually minor and the bands do not increase significantly with time, Fig. S2 (Supporting Information). Boerio *et al.* studied the rate of degradation of thin PS films and reported that it is substantial above nominal laser powers of 50 mW and that the increase in film thickness inhibited the degradation reaction.[16] In our experiments, we use much lower laser powers (7.5 mW) whereas the presence of a second polymeric film increases the total thickness of system thus protecting the substrate and the lower film. In summary, the gold SERS substrate employed behaves rather well in terms of spectral quality, with minimum polymer degradation and very good performance even at high temperature.

Diffusion between polymers films was promoted by annealing the bilayer above the $T_g$ of the polymers, that is, with the polymers in the melt state. To monitor the interdiffusion process, Raman spectra were collected periodically, while the specimen was annealed. Figure 4 shows the time evolution of normalized SERS spectra of the dPS/PS system (80 nm/80 nm), annealed at several temperatures above 100 °C, the $T_g$ of PS and dPS. Upon annealing, diffusion is activated enabling PS chains to reach the hot spot of the SERS substrate. This is evidenced by the progressive increase in the intensity of the characteristic PS band at 1000 cm$^{-1}$ over time. Figure 4(A) shows the experiment carried out at 150 °C. Initially, the SERS spectrum only shows spectral features of the dPS

component (peak at 960 cm$^{-1}$) but after about 30 min of annealing, a small contribution of PS starts to show up and to slowly increase. The same is observed at 160 °C (Fig. 4(B)), but at a slightly higher rate. At 175 °C, the rate of appearance of the peak at 1000 cm$^{-1}$ is even faster. The spectrum at 120 min shows that the two tracer peaks have comparable intensity, which would indicate that the overall polymer blend composition detected in the substrate hotspot is about 50 wt%. This result is consistent with the fact that both polymer layers have similar thicknesses so diffusion at high temperature and sufficiently long annealing times should produce an equilibrium composition profile with an average value of about 50 wt%. Figure 4(D) shows results of a sample built with the PS film on the bottom and the dPS film on top, that is, an inverted geometry. Remarkably, we observe that it is now dPS the emerging component, at a similar rate observed in the experiment shown in Fig. 4(C). Overall, we found excellent data reproducibility and spectral quality in relatively short acquisition times, allowing dynamic and reliable data acquisition.

We now address the problem of translating those spectral changes to a reliable parameter to quantify polymer diffusion. We interpret that the SERS experiment is capturing a cumulative weight fraction (*cwf*) over all the polymer chains that have been effectively detected in the hot spot or detection zone. All these convoluted contributions are reflected in the Raman spectrum measured at a given diffusion time. From the Raman spectrum, one can straightforwardly obtain a corresponding weight fraction for PS or dPS, using the calibration curve explained in the experimental part. We remind here the cumulative character of *cwf* despite the fact the calibration curve yields a single value of PS (or dPS) weight fraction.

Figure 5 shows the time evolution of *cwf* for PS species, obtained from each Raman spectrum and the calibration curve, for several annealing temperatures. In most of the plots, results of at least two independent experiments have been shown, represented with different symbols. We see that the PS *cwf* profiles show a behavior characteristic of diffusion, where mixing evolves rapidly at the beginning, to progressively slow down as the system approaches to its equilibrium state. As discussed above, considering that dPS and PS films have similar thickness, the expected weight fraction at equilibrium value should be around 0.5. Clearly, at all the temperatures, the experimental data tend toward that value, although it is only achieved in the experiments conducted at the higher temperature (175 °C). Figure 5(D) includes the *cwf* profile of the sample with inverted geometry, a mirror image of that regular, which is consistent with a diffusive process.

We can estimate the range of diffusion coefficients that the technique is sensing as a way to put all these results in adequate perspective. As dPS and PS have the same molecular weight and $T_g$, a simple Fick law with constant diffusion coefficient ($D$) can precisely describe the mass transport process across the dPS–PS interface. As a first approximation, characteristic diffusion distances ($L$) for one-dimensional diffusion are given by[21]:

$$L = 2(Dt)^{1/2} \qquad (1)$$

where $t$ represents the diffusion time and $D$ the binary diffusion coefficient. If we consider the experiment carried out at 175 °C, Fig. 5 (D) shows that the bilayer reaches its equilibrium composition in about 1 h. Assuming that each bilayer has a nominal thickness of about 80 nm, PS chains have to be diffused on that order distances. Making $L = 80$ nm and $t = 1$ h, Eqn (1) yields value of $D$ of $7.0 \times 10^{-14}$ cm$^2$/s, very close to that of $1.0 \times 10^{-13}$ cm$^2$/s reported
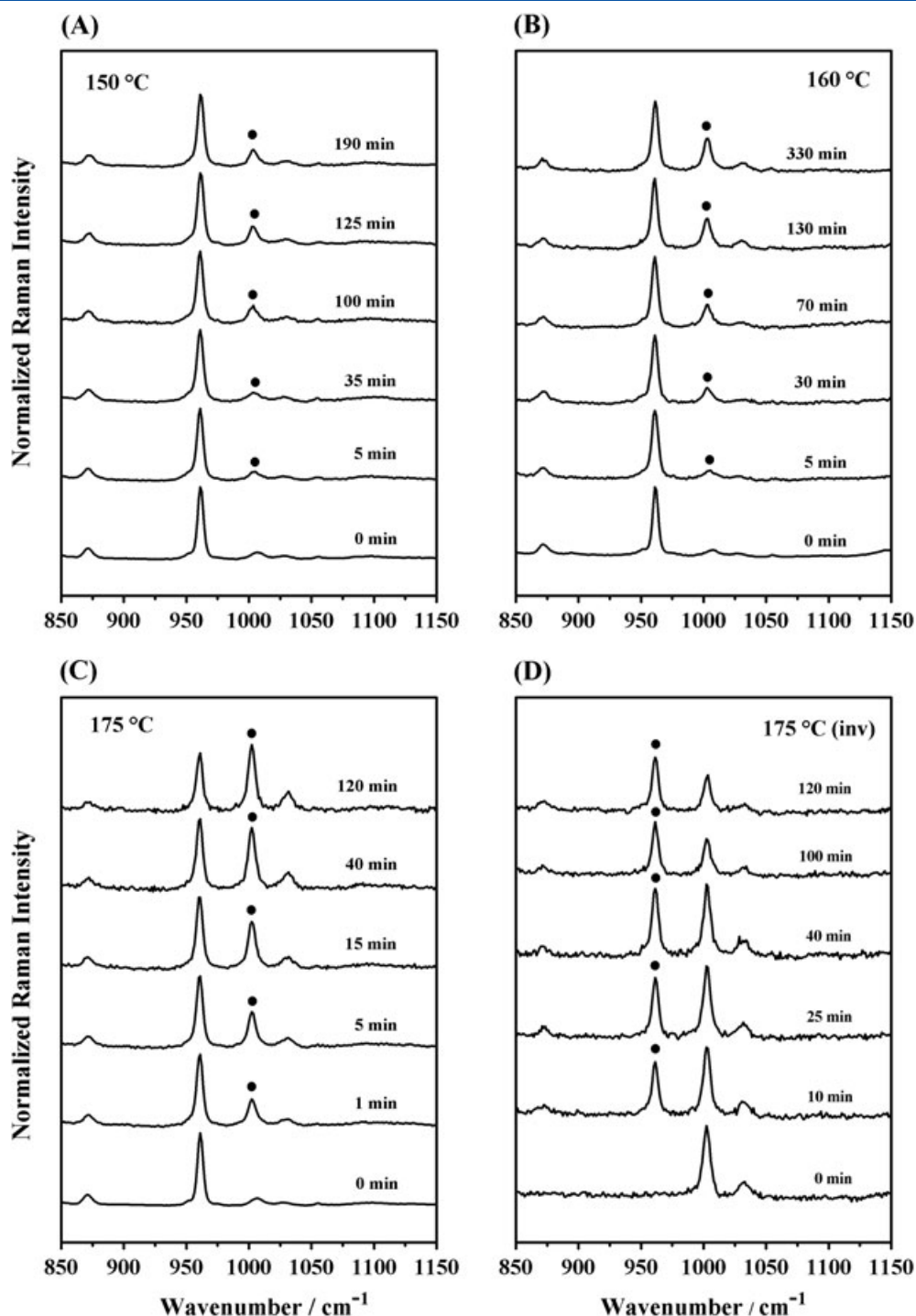
**Figure 4.** Temporal evolution of SERS spectra from a bilayer system PS/dPS (80 nm/80 nm) at: (A) 150 °C; (B) 160 °C; (C) 175 °C; (D) 175 °C, inverted system.

in the literature for the dPS–PS system at 175 °C. A similar argument applied to the data at 150 °C indicates that the kinetics of mixing is characterized by a $D$ of $2.7 \times 10^{-15}$ cm$^2$/s, close to that of $5 \times 10^{-15}$ cm$^2$/s reported in similar conditions.

Another proof of data consistency can be found from the analysis of the temperature response of the experiment. Overall, good data superposition in appropriate representations is used to support of well-behaved and consistent diffusion data. For instance, plotting the data in a $\sqrt{(D/D_0)}\, t/h$ $x$-scale should yield a single master curve for the case of Fickean diffusion, where $h$ represents the initial

slab thickness, $D$ the diffusion coefficient at $T$, $D_0$ that at a reference temperature $T_0$ and $t$ the elapsed time.[21] We have used this representation for our PS $cwf$ data collected at different times, for several temperatures, as shown in Fig. 6. Let us briefly explain how the plot was approached. In principle, all we need to build the master curve are $D$ values at several temperatures and a value of $h$. Although $D$ values can be estimated from our experiment via Eqn (1), this equation is only valid for one-dimensional mass transport, whereas diffusion is most likely multidimensional because of the geometry of the substrate. Instead of using estimated $D$ values to build the
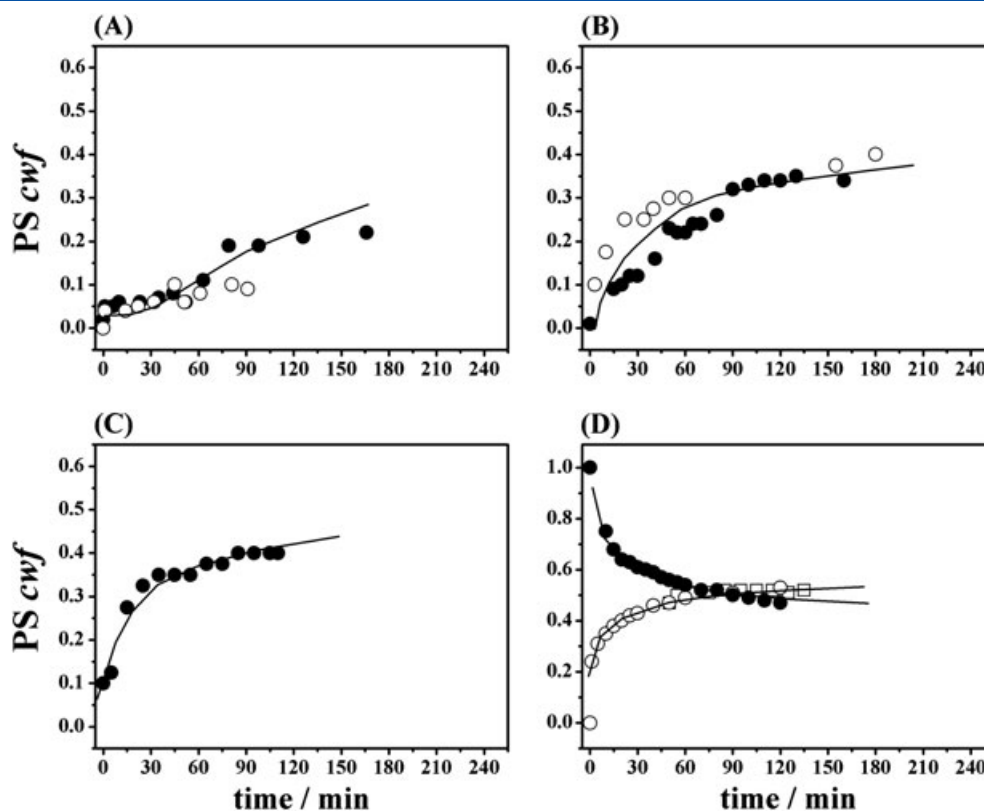
**Figure 5.** Evolution of PS cumulative mass fraction (PS *cwf*) profiles. Samples held at: (A) 150 °C; (B) 160 °C; (C) 165 °C; (D) 175 °C, regular and inverted system. Solid lines were drawn as a guide.
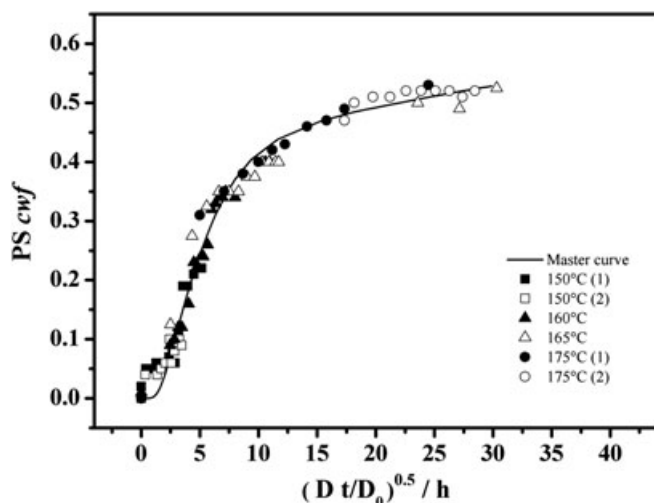


**Figure 6.** Master curve built taken the data at 160 °C as reference, see details in the text.

plot, we use the quotient $D/D_0$ as a fitting parameter that one varies up to obtain good superposition with the data at $T_0$. Following this approach, the set of data at 160 °C was taken as a reference temperature, so $D/D_0 = 1$ for this case. For the other temperatures, rescaling factors $D/D_0$ were individually obtained, as those that yield good superposition with the data at 160 °C. The value of $h$ was assumed to be the same for all the samples (80 nm). We see from Fig. 6 that the whole set of data can be very well superposed onto a single master curve. Some lack of superposition may be

attributed to small differences in layer thickness, assumed to be the same for all the bilayers. Also important, the rescaling factors (or quotient $D/D_0$) have an important physical meaning as they represent the relative change of diffusivity with temperature. They can be plot in Arrhenius fashion, see Fig. S3 (Supporting Information), to obtain activation energies ($E_a$) for the diffusive process. From the slope of the plot, we obtain $E_a = 48.93 \pm 1.5$ kcal/mol, very close to that predicted for this system in the same temperature range (47 kcal/mol),[22,23] which indicates that the experiment is correctly sensing the dependence of diffusion kinetics with temperature. The very good data superposition observed and the consistent values of the temperature dependency of the shift factors are taken as strong support for thermally activated polymer diffusion process.

## Conclusions

We have described the implementation of a relatively simple setup based on SERS to monitor the process of chain diffusion between two polymeric films. The setup yielded very good data quality in a reproducible fashion and enabled reliable data acquisition even at high temperature. The evolution of spectral features is consistent with mixing between polymer films at nanometer scale. The Raman signal arising from polymer chains initially located 80 nm further from the surface of the metallic substrate increases with time indicating that they have effectively diffused up to reach the detection zone close to the SERS substrate. The experiment provides a whole picture of the mixing kinetics and captures very well the evolution of the process up to the equilibrium state. The activation energy that characterizes the temperature response of diffusion is in very

good agreement with already published diffusion data. The characteristics diffusion distances assessed by the experiment, in the order of tens of nanometers, indicate that the experiment is sensing diffusion coefficients in the range $10^{-13}$–$10^{-15}$ cm$^2$/s, certainly without precedent in Raman microscopy. Smaller diffusion coefficients could be assessed by reducing film thickness or by tuning substrate geometry with the aim of reducing the dimensions of the substrate hotspot.

Overall, SERS experiments provide a powerful and reliable experimental platform to characterize polymer interdiffusion without the need of chemical labeling. Further work addressing both, the multidimensionality of the diffusion process and a realistic sizing of the hotspot through rigorous numerical simulation of plasmonic effects, is currently underway, with the aim of obtaining instantaneous diffusion coefficients by data fitting and a quantitative point-by-point characterization of the evolution of the diffusion process. Applications of SERS to the study of chain dynamics in the presence of nanoparticles, nanowires or nanotubes may be useful to deeply understand transport properties in advanced polymer-based nanocomposite materials.

## References

[1] R. J. Composto, E. J. Kramer, D. M. White, *Macromolecules* **1988**, *21*, 2580.
[2] R. A. L. Jones, J. Klein, A. M. Donald, *Nature* **1986**, *321*, 161.
[3] P. F. Nealey, R. E. Cohen, A. S. Argon, *Polymer* **1995**, *36*, 3687.
[4] T. E. Shearmur, A. S. Clough, D. W. Drew, M. G. D. van der Grinten, R. A. L. Jones, *Macromolecules* **1996**, *29*, 7269.
[5] J. K. Oh, J. P. Tomba, X. Ye, R. Eley, J. Rademacher, R. Farwaha, M. A. Winnik, *Macromolecules* **2003**, *36*, 5804.
[6] D. Wang, X. Liang, T. P. Russell, K. Nakajima, *Macromolecules* **2014**, *47*, 3761.
[7] Q. Gu, X. Wang, P. Sun, D. Zhou, G. Xue, *Soft Matter* **2011**, *7*, 691.
[8] N. Everall, *Appl. Spectrosc.* **2009**, *69*, 245.
[9] J. P. Tomba, J. M. Carella, J. M. Pastor, *Macromolecules* **2009**, *42*, 3565.
[10] A. C. De Luca, G. Rusciano, G. Pesce, S. Caserta, S. Guido, A. Sasso, *Macromolecules* **2008**, *41*, 5512.
[11] L. Xue, W. Li, G. G. Hoffmann, J. G. P. Goossens, J. Loos, G. de With, *Macromolecules* **2011**, *44*, 2852.
[12] B.-S. Yeo, E. Amstad, T. Schmid, J. Stadler, R. Zenobi, *Small* **2009**, *5*, 952.
[13] P. P. Hong, F. J. Boerio, S. D. Smith, *Macromolecules* **1993**, *26*, 1460.
[14] Renishaw Diagnostics. "Klarite—Substrates for Surface Enhanced Raman Scattering" Application Note. **May 2010**. http://www.renishawdiagnostics.com
[15] J. P. Tomba, E. De La Puente, J. M. Pastor, *J. Polym. Sci. Polym. Phys.* **2000**, *38*, 1013.
[16] P. P. Hong, F. J. Boerio, S. J. Clarson, S. D. Smith, *Macromolecules* **1991**, *24*, 4770.
[17] J. R. Anema, A. G. Brolo, A. Felten, C. Bittencourt, *J. Raman Spectrosc.* **2010**, *41*, 745.
[18] K. C. Vernon, T. J. Davis, F. H. Scholes, D. E. Gómez, D. Lau, *J. Raman Spectrosc.* **2010**, *41*, 1106.
[19] J. Li, X. Xu, Y. Wang, M. Wang, Z. Dong, W. Tian, J. Sun, C. Zhang, B. Wang, *J. Raman Spectrosc.* **2012**, *43*, 863.
[20] R. S. Venkatachalam, F. J. Boerio, M. R. Carnevale, P. G. Roth, *Appl. Spectrosc.* **1988**, *42*, 1207.
[21] J. Crank, *The Mathematics of Diffusion*, 2$^{nd}$ ed., Oxford, Great Britain, **2011**.
[22] P. Lomellini, *Polymer* **1992**, *33*, 4983.
[23] P. F. Green, E. J. Kramer, *Macromolecules* **1986**, *19*, 1108.

## Supporting information

Additional supporting information may be found in the online version of this article at the publisher's web site.